IEEE Access
Multidisciplinary | Rapid Review | Open Access Journal

Date of publication xxxx 00, 0000, date of current version xxxx 00, 0000.

Digital Object Identifier 10.1109/ACCESS.2021.Doi Number

Detection Method of Focal Plane Arrays with Noise Suppression for Optical Communications

XIAOYAN WANG[1], YUNING WANG[2], LI LI[1], JIANHUA ZHANG[1], ZHOUSHI YAO[1], CHANGZHI XU[1], and YI JIN[1]

[1]China Academy of Space Technology (Xi'an), 504 East Chang'an Street, Xi'an, Shaanxi, China
[2]Xi'an Jiaotong University, 28 West Xianning Street, Xi'an, Shaanxi, China

Corresponding author: Xiaoyan Wang (e-mail:1993969646@ qq.com) and Yuning Wang (e-mail:wangyn369369@163.com).

"This work was supported under grants."

ABSTRACT In many optical communication systems, in order to make the optical networking convenient and meet the application requirements, the optical terminals need to work in the same band and at the extremely closely adjacent working wavelengths. In practice, due to the light reflection and scattering of the wireless channels with the suspended particles, parts of the emitted optical signals will be reflected to the focal plane array (FPA). On the other hand, because the bandwidth of practical optical filters cannot be made narrow enough, or the sensitivity of FPAs is usually very high, the isolation between the transmitting and receiving optical paths in the terminal cannot be made high enough even if the optical filtering are used. Both the received optical signal from the remote terminal and the transmitted optical signal reflected by the terminal or wireless channels will be detected by the FPA at the same time. The reflected optical signal will interfere with the detection of the received optical signals from the far end, which seriously reduces the detection performance and the accuracy of the light spot centroid calculation. This paper proposes an integral control and increase-decrease counting statistical method for FPAs to eliminate the influence of the reflected optical signal on the signal detection and the noise mean value in the mean value of the total detection signal. The detection sensitivity of the received signal from the remote terminal, the isolation of the transmitting and receiving paths and the accuracy of the light spot centroid calculation are improved by this method. The Cramer-Rao lower bound is calculated and analyzed. In addition, the integral control and increase-decrease counting statistical algorithm is verified by the two software co-simulation, and the simulation results are given to illustrate the feasibility and performance of this method.

INDEX TERMS Optical communications, focal plane array detection, noise suppression

I. INTRODUCTION

Optical communication uses light as the carrier to transmit information and has many advantages as a promising means, such as higher data rate, smaller beam width, better transmission confidentiality and stronger anti-electromagnetic interference ability, etc. With the continuous development and maturity of optical communication technology in recent years, many demonstration experiments of laser links from near earth to lunar distance have been successful, which greatly promote the development of high-speed space laser communications. In order to meet the increasing needs of human beings, space optical communication technology is gradually applied to various fields, such as near earth optical communication, deep space exploration, underwater optical communication, terrestrial free space optics, etc.

In a variety of optical communication applications, the terminal usually uses the focal plane array (FPA) to detect the optical signals to complete the integration of telecommunication, acquisition, tracking, pointing, ranging and other functions. For example, the space-borne optical communication terminal uses the FPA to detect the optical signal. Each pixel of the FPA receives the incident optical signal respectively, carries out photoelectric detection and outputs the gray value of the received signal for the pointing, acquisition and tracking (PAT) function of the terminal. The FPA can be the photodiode PIN detector array, avalanche photodiode (APD) detector array, Geiger mode APD detector array, etc, working in visible light, near infrared, mid infrared

or far infrared bands, and its materials can be silicon, InGaAs, HgCdTe, etc.

FPAs have the following advantages for optical communications: (a) The detection sensitivity of FPAs is usually very high and can achieve the high accuracy of the spot centroid calculation. For example, the detection sensitivity of InGaAs FPAs is about -80dBm～-85dBm, while the detection sensitivity of four quadrant detector (QD) is about -65dbm～-70dBm. (b) The FPA is composed of multiple pixels, which is easy to be expanded in scale, and can achieve a larger field of view (FOV) by adding pixels for acquisition. It can also achieve spot tracking by the signal detection of different pixels, so using one single FPA device can achieve both acquisition and tracking at the same time. (c) The space intervals between FPA pixels are small comparing with those of QD, and there is no need to defocus the received spot to achieve the FPA signal detection, which will decrease the detection sensitivity and increase the equipment complexity.

In practical applications, the FPA in optical terminals will receive a variety of noises. The main noise sources include the following: (1) Due to the low isolation of the transmitting and receiving paths in the optical terminal, part of the transmitted light is reflected and detected by the FPA, and interferes with the received signal detection. (2) During the application of optical terminals, due to the external dirt, dust, unknown obstructions on the mirror surface of the telescope and other reasons, part of the transmitted optical signal can be reflected and detected by the FPA resulting in the detection noise. (3) Due to the scattering and reflection of the optical signal by various airborne particles in the wireless channel, especially in the turbid underwater channel or the atmospheric channel, part of the transmitted signal can be reflected and becomes the part of incident signals. (4) The FPA detector noises include the shot noise, dark current noise, thermal noise and readout circuit noise of FPA devices, etc.

On the one hand, the power of the transmitted optical signal is usually very high in order to meet the need of the long-distance communication, so the reflected optical signal can be a big noise contribution. On the other hand, the device states of optical terminals in use change continually. For example, the cleanliness of the telescope mirror or the pointing ahead angle of the transmitted optical signal changes gradually in use, so the intensity and spatial distribution of the reflected optical signal change randomly, continuously and slowly compared with the communication data. These random noises seriously reduce the performance of the received signal detection and the accuracy of light spot centroid calculation.

In many optical communication systems, in order to make the optical networking convenient and meet the system application requirements, the optical terminals need to work in the same band and at the extremely closely adjacent working wavelengths. For example, the working wavelengths of the two inter-satellite optical terminals are in the 1550nm band, and the wavelength interval is less than 1nm. In some practical and advanced applications, because the bandwidth of the optical filter cannot be made narrow enough, the optical communication terminal cannot perform satisfactory isolation of the receiving and transmitting paths by only using the traditional filtering. For example, the bandwidth of the narrow band optical filter in front of the FPA can only be 2-3nm in practice. Thus the received optical signal from the remote terminal and the transmitted optical signal reflected by the terminal or the wireless channels are both detected by the FPA at the same time. The reflected optical signal, which contributes to the noise source in the signal detection, seriously degrades the performance of the optical signal detection and reduces the accuracy of the spot centroid calculation.

In order to solve this noise interference problem of FPAs, this paper proposes a method of the integral control and increase-decrease counting statistical algorithm (ICIDC). In this ICIDC method, on the one hand, the special designs of different transmitted signal formats are adopted for the different transmitters, and the special design of the corresponding integral control signal of the FPA is adopted at the receiver. In addition, the signal detection and processing based on the increase-decrease counting statistical algorithm is used to eliminate the noise effectively. On the other hand, the noise mean value in the mean value of the total detection signal is eliminated by the increase-decrease counting statistical algorithm, so as to greatly eliminate the noise influence on the detection signal, and to effectively improve the sensitivity of the received signal detection, the isolation of the transmitting and receiving paths and the accuracy of the spot centroid calculation.

On the base of the principle of statistical signal detections, the composition and characteristics of the detection signals and noises are analyzed in this paper. The statistical models of FPA signal detections are established, and the specific implementation scheme by using the ICIDC statistical algorithm is designed. The performance of this method is analyzed and the Cramer-Rao lower bound is calculated. At the same time, the co-simulation of the OptiSystem and MATLAB software is implemented, and the output signal waveforms and calculation results are obtained. These calculation results fully prove the feasibility and performance of this ICIDC method.

II. SYSTEM OVERVIEW AND SIGNAL DESIGN

The implementation scheme of the ICIDC statistical algorithm for FPAs includes three parts: (a) At the transmitter, the special designs of differently modulated signal formats are adopted. The emitted optical signals from the different optical terminals are modulated with different frequencies, and work in the same band and at the closely adjacent wavelength. (b) At the receiver, the special design of the integral control signal for the FPA is adopted, so each pixel detector of a single FPA with the same one integral

control signal can output different integral results for the two optical signals with the differently modulated frequencies. (c) At the receiver, the ICIDC statistical algorithm is used for each pixel detector output to eliminate the influences of the reflected optical signal and the device noises, in order to effectively improve the detection performance, the path isolation and the centroid calculation accuracy, etc. The system diagram of one application is shown in Fig. 1 as follow.

A. FORMAT DESIGN OF MODULATED SIGNALS $S_1(t)$ AND $S_2(t)$:

In one communication system, the transmitted optical signal from the terminal A is at the wavelength of 1550nm and is modulated by the signal $S_1(t)$ with the frequency f_1 and the equivalent average amplitude I_1. The transmitted optical signal from the terminal B is at the wavelength of 1551nm and is modulated by the signal $S_2(t)$ with the frequency f_2 and the effective average amplitude I_2. The $S_1(t)$ and $S_2(t)$ are the periodic signals of the On-off Keying format and $f_1 \neq f_2$. In each $S_1(t)$ period $[0, T_1)$ and $T_1 = \left(\frac{1}{f_1}\right)$, the FPA integral output of $S_1(t)$ during the time interval of $[0, pT_1)$ is different from that of $S_1(t)$ during the time interval of $[pT_1, T_1)$ and can be represented as $\frac{uI_1}{f_1}$ and $\frac{vI_1}{f_1}$ respectively. In each $S_2(t)$ period $[0, T_2)$ and $T_2 = \left(\frac{1}{f_2}\right)$, the FPA integral output of $S_2(t)$ during the time interval of $[0, p'T_2)$ is different from that of $S_2(t)$ during the time interval of $[p'T_2, T_2)$ and can be represented as $\frac{u'I_2}{f_2}$ and $\frac{v'I_2}{f_2}$ respectively. The signal $S_1(t)$ and $S_2(t)$ can be represented by (1) as follow, where $u + v = 1$, $u \neq v$, $u' + v' = 1$, $u' \neq v'$, $u \in [0,1]$, $v \in [0,1]$, $u' \in [0,1]$, $v' \in [0,1]$, $f_1 \neq f_2$, $p \in (0,1)$ and $p' \in (0,1)$. u, v, u', v', p, p', I_1 and I_2 are the positive real numbers. M_1, M_2, f_1, f_2 and l are the positive integers.

$$\begin{cases} \int_{\frac{l(2M_1+1)}{f_1}}^{\frac{(l+1)(2M_1+1)}{f_1}} S_1(t)\,dt = \int_{\frac{(l+1)(2M_1+1)}{f_1}}^{\frac{(l+2)(2M_1+1)}{f_1}} S_1(t)\,dt = \frac{(2M_1+1)I_1}{f_1} \\ \int_{\frac{l(2M_1+1)}{f_1}}^{\frac{l(2M_1+1)+M_1}{f_1}} S_1(t)\,dt = \int_{\frac{(l+1)(2M_1+1)-M_1}{f_1}}^{\frac{(l+1)(2M_1+1)}{f_1}} S_1(t)\,dt = \frac{M_1 I_1}{f_1} \\ \int_{\frac{l}{f_1}}^{\frac{l+p}{f_1}} S_1(t)\,dt = \frac{uI_1}{f_1} \neq \int_{\frac{l+p}{f_1}}^{\frac{l+1}{f_1}} S_1(t)\,dt = \frac{vI_1}{f_1} \\ \int_{\frac{l(2M_2)}{f_2}}^{\frac{(l+1)(2M_2)}{f_2}} S_2(t)\,dt = \int_{\frac{(l+1)(2M_2)}{f_2}}^{\frac{(l+2)(2M_2)}{f_2}} S_2(t)\,dt = \frac{2M_2 I_2}{f_2} \\ \int_{\frac{l(2M_2)}{f_2}}^{\frac{l(2M_2)+M_2}{f_2}} S_2(t)\,dt = \int_{\frac{(l+1)(2M_2)-M_2}{f_2}}^{\frac{(l+1)(2M_2)}{f_2}} S_2(t)\,dt = \frac{M_2 I_2}{f_2} \\ \int_{\frac{l}{f_2}}^{\frac{l+p'}{f_2}} S_2(t)\,dt = \frac{u'I_2}{f_2} \neq \int_{\frac{l+p'}{f_2}}^{\frac{l+1}{f_2}} S_2(t)\,dt = \frac{v'I_2}{f_2} \end{cases} \quad (1)$$

B. FORMAT DESIGN OF INTEGRAL CONTROL SIGNAL $S_{int}(t)$

In this ICIDC method, the multi-frame joint design is adopted for the FPA integral control signal $S_{int}(t)$, so the optical terminal can use the pixel detectors of a single FPA and the same one $S_{int}(t)$ to differentiate the two incident optical signals modulated by $S_1(t)$ and $S_2(t)$ with the two different frequencies f_1 and f_2, in order to obtain their equivalent average amplitudes I_1 and I_2 respectively and more precisely. In addition, the mean value of noises can be removed from the calculation formulas of I_1 and I_2 and the noise influence can be suppressed.

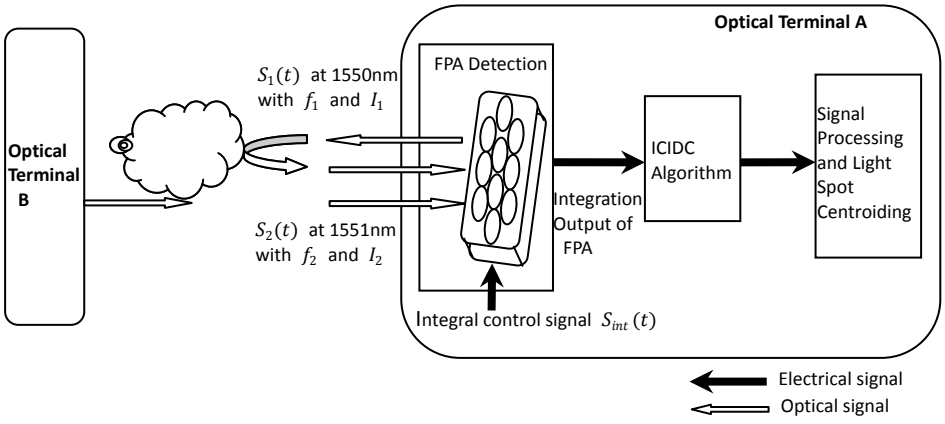

FIGURE 1. System overview

This article has been accepted for publication in a future issue of this journal, but has not been fully edited. Content may change prior to final publication. Citation information: DOI 10.1109/ACCESS.2021.3110968, IEEE Access

The main design of this FPA integral control signal $S_{int}(t)$ includes the following parts: (1) There are several frames in each period of the periodic $S_{int}(t)$ and there are several time segments in each frame of this $S_{int}(t)$. In each time segment of this $S_{int}(t)$, the number of periods of one incident modulated signal (e.g. $S_1(t)$), which are integrated by the FPA, is a positive non-integer, and the number of periods of the other incident modulated signal (e.g. $S_2(t)$), which are integrated by the FPA, is a positive integer. (2) For both of the two incident modulated signals (e.g. $S_1(t)$ and $S_2(t)$), the integral output of one FPA pixel detector for the former part of one signal period (e.g. $[0, pT_1)$ or $[0, p'T_2)$) is different from that for the latter part of one signal period (e.g. $[pT_1, T_1)$ or $[p'T_2, T_2)$). One of the multi-frame joint schemes for the integral control signal $S_{int}(t)$ is proposed and the integral output of one FPA pixel detector is analyzed as follow.

1) INTEGRAL CONTROL SIGNAL $S_{int}(t)$

The FPA integral control signal $S_{int}(t)$ is a periodic signal modulated as the On-off Keying format and each $S_{int}(t)$ period includes 4 frames, which are represented as the R frame, the $(R+1)$ frame, the $(R+2)$ frame and the $(R+3)$ frame with the frame time $T_{frame} = \frac{1}{f_{frame}}$, where R is a positive odd number. The integral operation is enabled when $S_{int}(t) = 1$ and the integral operation is disabled when $S_{int}(t) = 0$.

During the frame time T_{frame} of the R frame and the $(R+1)$ frame, there are K consecutive integral time segments of $\left(\frac{i(2M_1+1)}{f_1}, \frac{(i+1)(2M_1+1)}{f_1}\right)$ or $\left(\frac{i(2M_2)}{f_2}, \frac{(i+1)(2M_2)}{f_2}\right)$ and $T_{frame} = K\left(\frac{2M_1+1}{f_1}\right) = K\left(\frac{2M_2}{f_2}\right)$, where $i = 0,1,2 \ldots (K-1)$. In addition, there is an integral time $T_{integral}$ in each T_{frame} of the R frame and the $(R+1)$ frame and $T_{integral} \le T_{frame}$, and there are J integral time segments in each $T_{integral}$, $T_{integral} = J\left(\frac{2M_1+1}{f_1}\right) = J\left(\frac{2M_2}{f_2}\right)$ and $J \le K$ because of the reset time of the FPA device in practice. During the frame time T_{frame} of the $(R+2)$ frame and the $(R+3)$ frame, there are K' consecutive integral time segments of $\left(\frac{i'(2M_3+1)}{f_1}, \frac{(i'+1)(2M_3+1)}{f_1}\right)$ or $\left(\frac{i'(2M_4)}{f_2}, \frac{(i'+1)(2M_4)}{f_2}\right)$ and $T_{frame} = K'\left(\frac{2M_3+1}{f_1}\right) = K'\left(\frac{2M_4}{f_2}\right)$, where $i' = 0,1,2 \ldots (K'-1)$. In addition, there is an integral time $T_{integral}{}'$ in each T_{frame} of the $(R+2)$ frame and the $(R+3)$ frame and $T_{integral}{}' \le T_{frame}$, and there are J' integral time segments in each $T_{integral}{}'$, $T_{integral}{}' = J'\left(\frac{2M_3+1}{f_1}\right) = J'\left(\frac{2M_4}{f_2}\right)$ and $J' \le K'$ because of the FPA device reset time in practice. M_3, M_4, K, K', J and J' are the positive integers.

2) R AND $(R+1)$ FRAME DESIGN

In the R frame, the FPA detects and outputs the integral of the incident signals including $S_1(t)$ and $S_2(t)$ during the time segment of $\left(\frac{i(2M_1+1)}{f_1}, \frac{i(2M_1+1)+M_5+p}{f_1}\right)$. The integral output of one pixel detector for $S_1(t)$ in this time segment includes a positive non-integer number of the $S_1(t)$ signal period and is expressed as $\frac{(M_6+u)I_1}{f_1}$. The integral output of one pixel detector for $S_2(t)$ in this time segment includes a positive integer number of the $S_2(t)$ signal periods and is expressed as $\frac{M_8 I_2}{f_2}$.

In the $(R+1)$ frame, the FPA detects and outputs the integral of the incident signals including $S_1(t)$ and $S_2(t)$ during the time segment of $\left(\frac{(i+1)(2M_1+1)-M_5-p}{f_1}, \frac{(i+1)(2M_1+1)}{f_1}\right)$. The integral output for $S_1(t)$ in this time segment includes a positive non-integer number of the $S_1(t)$ signal period and is expressed as $\frac{(M_7+v)I_1}{f_1}$. The integral output for $S_2(t)$ in this time segment includes a positive integer number of the $S_2(t)$ signal periods and is expressed as $\frac{M_9 I_2}{f_2}$, where $M_6 + u \neq M_7 + v$. M_5, M_6, M_7, M_8 and M_9 are the positive integers. The FPA output signal can be modeled as follow:

$$\begin{cases} \int_{\frac{i(2M_1+1)}{f_1}}^{\frac{(i+1)(2M_1+1)}{f_1}} S_1(t)\, S_{int}(t)dt = \int_{\frac{(i+1)(2M_1+1)}{f_1}}^{\frac{(i+2)(2M_1+1)}{f_1}} S_1(t) S_{int}(t)\, dt \\ \int_{\frac{i(2M_2)}{f_2}}^{\frac{(i+1)(2M_2)}{f_2}} S_2(t)\, S_{int}(t)dt = \int_{\frac{(i+1)(2M_2)}{f_2}}^{\frac{(i+2)(2M_2)}{f_2}} S_2(t) S_{int}(t)\, dt \\ \int_{\frac{i(2M_1+1)}{f_1}}^{\frac{i(2M_1+1)+M_5+p}{f_1}} S_1(t) S_{int}(t)\, dt = \begin{cases} \frac{(M_6+u)I_1}{f_1} & for\ S_{int}(t) = 1\ and\ R\ frame \\ 0 & for\ S_{int}(t) = 0\ and\ (R+1)\ frame \end{cases} \\ \int_{\frac{(i+1)(2M_1+1)-M_5-p}{f_1}}^{\frac{(i+1)(2M_1+1)}{f_1}} S_1(t)\, S_{int}(t)dt = \begin{cases} 0 & for\ S_{int}(t) = 0\ and\ R\ frame \\ \frac{(M_7+v)I_1}{f_1} & for\ S_{int}(t) = 1 and (R+1)\ frame \end{cases} \\ \frac{(M_6+u)I_1}{f_1} \neq \frac{(M_7+v)I_1}{f_1} \\ \int_{\frac{i(2M_1+1)}{f_1}}^{\frac{i(2M_1+1)+M_8+p}{f_1}} S_2(t) S_{int}(t)\, dt = \begin{cases} \frac{M_8 I_2}{f_2} & for\ S_{int}(t) = 1\ and\ R\ frame \\ 0 & for\ S_{int}(t) = 0\ and\ (R+1)\ frame \end{cases} \\ \int_{\frac{(i+1)(2M_1+1)-M_5-p}{f_1}}^{\frac{(i+1)(2M_1+1)}{f_1}} S_2(t)\, S_{int}(t)dt = \begin{cases} 0 & for\ S_{int}(t) = 0\ and\ R\ frame \\ \frac{M_9 I_2}{f_2} & for\ S_{int}(t) = 1\ and\ (R+1)\ frame \end{cases} \end{cases} \quad (2)$$

3) $(R+2)$ AND $(R+3)$ FRAME DESIGN

In the $(R+2)$ frame, the FPA detects and outputs the integral of the incident signals including $S_1(t)$ and $S_2(t)$ during the time segment of $\left(\frac{i'(2M_3+1)}{f_1}, \frac{i'(2M_3+1)+M_{10}+p'}{f_1}\right)$. The integral output of one pixel detector for $S_1(t)$ in this time segment includes a positive integer number of the $S_1(t)$ signal periods and is expressed as $\frac{M_{11}I_1}{f_1}$. The integral output for $S_2(t)$ includes a positive non-integer number of the $S_2(t)$ signal periods and is expressed as $\frac{(M_{13}+u')I_2}{f_2}$.

In the $(R+3)$ frame, the FPA detects and outputs the integral of the incident signals including $S_1(t)$ and $S_2(t)$ during the time segment of $\left(\frac{(i'+1)(2M_3+1)-M_{10}-p'}{f_1}, \frac{(i'+1)(2M_3+1)}{f_1}\right)$. The integral output for $S_1(t)$ in this time segment includes a positive integer number of the $S_1(t)$ signal period and is expressed as $\frac{M_{12}I_1}{f_1}$. The integral output for $S_2(t)$ includes a positive non-integer number of the $S_2(t)$ signal periods and is expressed as $\frac{(M_{14}+v')I_2}{f_2}$, where $M_{13} + u' \neq M_{14} + v'$. M_{10}, M_{11}, M_{12}, M_{13}

and M_{14} are the positive integers. By the design of integral control signal $S_{int}(t)$, the formula $(M_8 - M_9)(M_{11} - M_{12}) \neq [(u - v) + (M_6 - M_7)][(u' - v') + (M_{13} - M_{14})]$ can be satisfied. The FPA output signal can be modeled as follow:

$$\begin{cases} \int_{\frac{i'(2M_3+1)}{f_1}}^{\frac{(i'+1)(2M_3+1)}{f_1}} S_1(t)\,S_{int}(t)dt = \int_{\frac{(i'+1)(2M_3+1)}{f_1}}^{\frac{(i'+2)(2M_3+1)}{f_1}} S_1(t)S_{int}(t)\,dt \\ \int_{\frac{i'(2M_4)}{f_2}}^{\frac{(i'+1)(2M_4)}{f_2}} S_2(t)\,S_{int}(t)dt = \int_{\frac{(i'+1)(2M_4)}{f_2}}^{\frac{(i'+2)(2M_4)}{f_2}} S_2(t)S_{int}(t)\,dt \\ \int_{\frac{i'(2M_3+1)}{f_1}}^{\frac{i'(2M_3+1)+M_{10}+p'}{f_1}} S_1(t)S_{int}(t)\,dt = \begin{cases} \frac{M_{11}I_1}{f_1} & for\ S_{int}(t)=1\ and\ (R+2)\ frame \\ 0 & for\ S_{int}(t)=0\ and\ (R+3)\ frame \end{cases} \\ \int_{\frac{(i'+1)(2M_3+1)}{f_1}}^{\frac{(i'+1)(2M_3+1)}{f_1}} S_1(t)\,S_{int}(t)dt = \begin{cases} 0 & for\ S_{int}(t)=0\ and\ (R+2)\ frame \\ \frac{M_{12}I_1}{f_1} & for\ S_{int}(t)=1\ and\ (R+3)\ frame \end{cases} \\ \frac{(M_{13}+u')I_2}{f_2} \neq \frac{(M_{14}+v')I_2}{f_2} \\ \int_{\frac{i'(2M_3+1)}{f_1}}^{\frac{i'(2M_3+1)+M_{10}+p'}{f_1}} S_2(t)S_{int}(t)\,dt = \begin{cases} \frac{(M_{13}+u')I_2}{f_2} & for\ S_{int}(t)=1\ and\ (R+2)\ frame \\ 0 & for\ S_{int}(t)=0\ and\ (R+3)\ frame \end{cases} \\ \int_{\frac{(i'+1)(2M_3+1)}{f_1}}^{\frac{(i'+1)(2M_3+1)}{f_1}} S_2(t)\,S_{int}(t)dt = \begin{cases} 0 & for\ S_{int}(t)=0\ and\ (R+2)\ frame \\ \frac{(M_{14}+v')I_2}{f_2} & for S_{int}(t)=1 and (R+3)\ frame \end{cases} \end{cases} \quad (3)$$

III. MODELING AND ALGORITHMS

In the ICIDC method of the FPA signal detection and processing, by using differently modulated signal designs for the different optical terminals, and combining with the multi-frame joint design of integral control signals, as well as the increase-decrease counting statistical algorithm, the FPA pixel detector outputs differently for the two modulated incident signals. Therefore, the equivalent average amplitudes of the two incident signals e.g. I_1 and I_2, can be obtained respectively, and the interference signal and device noises are suppressed at the same time. This ICIDC can ultimately improve the optical signal detection performance and the spot centroid accuracy.

If the number of the incident signal periods that are integrated by the FPA is a positive integer, the synchronization between this signal and the integral control signal will not impact the integral output results because of the signal periodic properties. In this paper, it is assumed that the synchronization between the modulated incident signal and the integral control signal can be achieved. If the number of the incident signal periods that are integrated by the FPA is a positive non-integer. The detailed synchronization method is out of range of this paper and will discuss in the future.

A. MODELING AND ANALYSIS OF THE FPA SIGNAL DETECTION

Each pixel of the FPA outputs the integral electrical signal of the photoelectric detection at the frame frequency f_{frame}, which is expressed as the output sequence $y[n]$. According to the design of the modulated signals and the integral control signal, and the analysis of the FPA noise sources, the integral output part of the signals $S_1(t)$ and $S_2(t)$ for each pixel is the deterministic variable and the noise output part for each FPA pixel is the Gaussian-distributed random variable N_p, which can be represented as $N_p \sim Gaussian(m_p, {\sigma_p}^2)$ with the mean m_p and the variance ${\sigma_p}^2$. The total output sequence $y[n]$ for each pixel is also the random variable $y[n] \sim Gaussian(m_y, {\sigma_y}^2)$ with the mean m_y and the variance ${\sigma_y}^2 = {\sigma_p}^2$. Because each pixel detects the optical signal independently, the FPA outputs are the independent and identically distributed (i.i.d) Gaussian random variables.

The observation vector $\vec{\boldsymbol{Y}}$ is formed by the following expression:

$$\vec{\boldsymbol{Y}} = \begin{bmatrix} Y_1 & Y_2 & Y_3 & Y_4 & \dots & Y_q & Y_{q+1} & Y_{q+2} & Y_{q+3} & \dots & Y_{N_y} \end{bmatrix} \quad (4)$$

where $Y_\omega = \frac{1}{L}\sum_{h=0}^{L-1} y(N_y h + \omega)$, ω can be q, $(q+1)$, $(q+2)$ or $(q+3)$. $q \in \{1,5,9\dots,(N_y-3)\}$, $(q+1) \in \{2,6,10\dots,(N_y-2)\}$, $(q+2) \in \{3,7,11\dots,(N_y-1)\}$, $(q+3) \in \{4,8,12\dots,N_y\}$. $N_y = 4\mu$, N_y、L、μ and q are the positive integers. In each calculation, there are L periods in the output sequence $y[n]$ and there are N_y elements in each period of $y[n]$. By using the summation formula of Y_ω, the corresponding elements with the same sequence number in periods are added to form the variables Y_q, Y_{q+1}, Y_{q+2} and Y_{q+3}, and the observation vector $\vec{\boldsymbol{Y}}$ is formed finally. The diagram for the vector $\vec{\boldsymbol{Y}}$ construction is shown in Fig. 2 below.

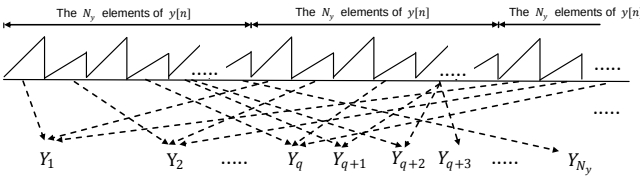

FIGURE 2. Diagram of the observation vector $\vec{Y}$ construction

The elements of the observation vector $\vec{\boldsymbol{Y}}$ are the i.i.d Gaussian-distributed random variables according to the central limit theorem in statistics and are obtained as follow:

$$\begin{cases} Y_q = \frac{uJI_1}{2f_1} + \left[\frac{JM_6}{2} + \alpha(K-J)(2M_1+1)\right]\frac{I_1}{f_1} + \left[\frac{JM_8}{2} + \alpha(K-J)2M_2\right]\frac{I_2}{f_2} + N_{b,q} \\ Y_{q+1} = \frac{vJI_1}{2f_1} + \left[\frac{JM_7}{2} + \alpha(K-J)(2M_1+1)\right]\frac{I_1}{f_1} + \left[\frac{JM_9}{2} + \alpha(K-J)2M_2\right]\frac{I_2}{f_2} + N_{b,(q+1)} \\ Y_{q+2} = \frac{u'J'I_2}{2f_2} + \left[\frac{J'M_{11}}{2} + \alpha'(K'-J')(2M_3+1)\right]\frac{I_1}{f_1} + \left[\frac{J'M_{13}}{2} + \alpha'(K'-J')2M_4\right]\frac{I_2}{f_2} + N_{b,(q+2)} \\ Y_{q+3} = \frac{v'J'I_2}{2f_2} + \left[\frac{J'M_{12}}{2} + \alpha'(K'-J')(2M_3+1)\right]\frac{I_1}{f_1} + \left[\frac{J'M_{14}}{2} + \alpha'(K'-J')2M_4\right]\frac{I_2}{f_2} + N_{b,(q+3)} \end{cases} \quad (5)$$

where $N_{b,q}$, $N_{b,(q+1)}$, $N_{b,(q+2)}$, $N_{b,(q+3)}$ are the output noises of the elements of the vector $\vec{\boldsymbol{Y}}$ for each pixel and are the Gaussian-distributed random variables, $Gaussian(m_b, {\sigma_b}^2)$ with the mean m_b and the variance ${\sigma_b}^2$ if the non-uniformity of the FPA pixels is very small and can be ignored. α and α' are the positive real number, $\alpha \in [0,1]$ and $\alpha' \in [0,1]$. The elements Y_q, Y_{q+1}, Y_{q+2} and Y_{q+3} are all the Gaussian-distributed random variables $Gaussian(m_Y, {\sigma_Y}^2)$ with the mean m_Y and the variance ${\sigma_Y}^2 = L\frac{{\sigma_p}^2}{L^2} = \frac{{\sigma_p}^2}{L}$.

The decision vector $\vec{\boldsymbol{F}} = [F_\beta \quad F_\gamma]$ can be formed as the following expression:

This article has been accepted for publication in a future issue of this journal, but has not been fully edited. Content may change prior to final publication. Citation information: DOI 10.1109/ACCESS.2021.3110968, IEEE Access

$$\begin{cases} F_\beta = \frac{1}{2\left(\frac{N_y}{4}\right)}\left(Y_1 - Y_2 + Y_5 - Y_6 + \cdots Y_q - Y_{q+1} \ldots + Y_{N_y-3} - Y_{N_y-2}\right) = \frac{1}{2}\left(Y_Q - Y_{Q+1}\right) \\ F_\gamma = \frac{1}{2\left(\frac{N_y}{4}\right)}\left(Y_3 - Y_4 + Y_7 - Y_8 + \cdots Y_{q+2} - Y_{q+3} \ldots + Y_{N_y-1} - Y_{N_y}\right) = \frac{1}{2}\left(Y_{Q+2} - Y_{Q+3}\right) \end{cases} \tag{6}$$

where Q and $(Q+2)$ are the positive odd number, $(Q+1)$ and $(Q+3)$ are the positive even number.

The calculation formulas are $Y_Q = \frac{1}{\left(\frac{N_y}{4}\right)}\sum_{j=0}^{\left(\frac{N_y}{4}-1\right)}\left(Y_{4j+1}\right)$, $Y_{Q+1} = \frac{1}{\left(\frac{N_y}{4}\right)}\sum_{j=0}^{\left(\frac{N_y}{4}-1\right)}\left(Y_{4j+2}\right)$, $Y_{Q+2} = \frac{1}{\left(\frac{N_y}{4}\right)}\sum_{j=0}^{\left(\frac{N_y}{4}-1\right)}\left(Y_{4j+3}\right)$ and $Y_{Q+3} = \frac{1}{\left(\frac{N_y}{4}\right)}\sum_{j=0}^{\left(\frac{N_y}{4}-1\right)}\left(Y_{4j+4}\right)$. According to the above noise analysis and the central limit theorem in statistics, for larger parameter L, the elements of the observation vector $\vec{\boldsymbol{Y}}$, namely Y_Q, Y_{Q+1}, Y_{Q+2} and Y_{Q+3}, are the i.i.d random variables and obey the Gaussian distribution, namely $Y_Q \sim Gaussian\left(m_Q, \frac{{\sigma_p}^2}{\left(\frac{N_y}{4}\right)_L}\right)$, $Y_{Q+1} \sim Gaussian\left(m_{Q+1}, \frac{{\sigma_p}^2}{\left(\frac{N_y}{4}\right)_L}\right)$, $Y_{Q+2} \sim Gaussian\left(m_{Q+2}, \frac{{\sigma_p}^2}{\left(\frac{N_y}{4}\right)_L}\right)$ and $Y_{Q+3} \sim Gaussian\left(m_{Q+3}, \frac{{\sigma_p}^2}{\left(\frac{N_y}{4}\right)_L}\right)$, where the mean values are m_Q, m_{Q+1}, m_{Q+2} and m_{Q+3} and the variances are $\frac{{\sigma_p}^2}{\left(\frac{N_y}{4}\right)_L}$, which can be expressed as follow respectively:

$$\begin{cases} E\left(Y_Q\right) = m_Q = \frac{uJI_1}{2f_1} + \frac{J}{2}\left(\frac{M_6 I_1}{f_1} + \frac{M_8 I_2}{f_2}\right) + \frac{\alpha(K-J)(2M_1+1)(I_1+I_2)}{f_1} + m_b \\ E\left(Y_{Q+1}\right) = m_{Q+1} = \frac{vJI_1}{2f_1} + \frac{J}{2}\left(\frac{M_7 I_1}{f_1} + \frac{M_9 I_2}{f_2}\right) + \frac{\alpha(K-J)(2M_1+1)(I_1+I_2)}{f_1} + m_b \\ E\left(Y_{Q+2}\right) = m_{Q+2} = \frac{u'J'I_2}{2f_2} + \frac{J'}{2}\left(\frac{M_{11} I_1}{f_1} + \frac{M_{13} I_2}{f_2}\right) + \frac{\alpha'(K'-J')(2M_3+1)(I_1+I_2)}{f_1} + m_b \\ E\left(Y_{Q+3}\right) = m_{Q+3} = \frac{v'J'I_2}{2f_2} + \frac{J'}{2}\left(\frac{M_{12} I_1}{f_1} + \frac{M_{14} I_2}{f_2}\right) + \frac{\alpha'(K'-J')(2M_3+1)(I_1+I_2)}{f_1} + m_b \\ Var\left(Y_Q\right) = Var\left(Y_{Q+1}\right) = Var\left(Y_{Q+2}\right) = Var\left(Y_{Q+3}\right) = \frac{{\sigma_p}^2}{\left(\frac{N_y}{4}\right)_L} \end{cases} \tag{7}$$

According to the above analysis, the decision variables F_β and F_γ of the vector $\vec{\boldsymbol{F}}$ also obey the i.i.d Gaussian distribution and can be expressed as $F_\beta \sim Gaussian\left(\frac{m_Q - m_{Q+1}}{2}, \frac{{\sigma_y}^2}{\left(\frac{N_y}{2}\right)_L}\right)$ and $F_\gamma \sim Gaussian\left(\frac{m_{Q+2} - m_{Q+3}}{2}, \frac{{\sigma_y}^2}{\left(\frac{N_y}{2}\right)_L}\right)$, where the variances of F_β and F_γ are the same ${\sigma_F}^2 = 2\frac{{\sigma_y}^2}{2^2} = \frac{{\sigma_y}^2}{\left(\frac{N_y}{2}\right)_L}$.

B. CALCULATION OF THE EQUIVALENT AVERAGE AMPLITUDES I_1 and I_2

For the FPA signal detection, it is assumed that the decision vector $\vec{\boldsymbol{F}} = [F_\beta \quad F_\gamma]$ is the ergodic random vector and the statistical mean values of the variables F_β and F_γ can be expressed by their temporal mean values respectively according to the statistical theories. The measured samples of the observation vector $\vec{\boldsymbol{F}}$ with the number Z_F can be represented as $\overrightarrow{\boldsymbol{F'}} = \begin{bmatrix} {F_{\beta,1}}' & {F_{\gamma,1}}' \\ {F_{\beta,2}}' & {F_{\gamma,2}}' \\ \cdots & \cdots \\ {F_{\beta,Z_F}}' & {F_{\gamma,Z_F}}' \end{bmatrix}$. The maximum likelihood (ML) estimator $\overrightarrow{\hat{\boldsymbol{I}}_{\boldsymbol{ML}}} = \left[\hat{I}_{1_{ML}} \quad \hat{I}_{2_{ML}}\right]$ of the vector $\vec{\boldsymbol{I}} = [I_1 \quad I_2]$ can be calculated by the following formula:

$$\begin{cases} \frac{\partial\{ln[p(\vec{F}|\vec{I})]\}}{\partial I_1}|_{I_1=\hat{I}_{1ML}} = 0 \\ \frac{\partial\{ln[p(\vec{F}|\vec{I})]\}}{\partial I_2}|_{I_2=\hat{I}_{2ML}} = 0 \end{cases} \tag{8}$$

where $\mathrm{p}(\cdot)$ is the probability.

By the design of the integral control signal $S_{int}(t)$, the formula $(M_8 - M_9)(M_{11} - M_{12}) \neq [(u-v) + (M_6 - M_7)][(u'-v') + (M_{13} - M_{14})]$ is satisfied. The mean values m_{F_β} and m_{F_γ} of the variables F_β and F_γ, and the statistical observation mean values $\overline{F_\beta}'$ and $\overline{F_\gamma}'$ are represented as follow.

$$\begin{cases} m_{F_\beta} = \frac{m_Q - m_{Q+1}}{2} = \frac{[(u-v)+(M_6-M_7)]JI_1}{4f_1} + \frac{[(M_8-M_9)]JI_2}{4f_2} \\ m_{F_\gamma} = \frac{m_{Q+2} - m_{Q+3}}{2} = \frac{[(u'-v')+(M_{13}-M_{14})]J'I_2}{4f_2} + \frac{(M_{11}-M_{12})J'I_1}{4f_1} \end{cases} \tag{9}$$

$$\begin{cases} \overline{F_\beta}' = \frac{1}{Z_F}\sum_{j=1}^{Z_F} {F_{\beta,j}}' \\ \overline{F_\gamma}' = \frac{1}{Z_F}\sum_{j=1}^{Z_F} {F_{\gamma,j}}' \end{cases} \tag{10}$$

where ${F_{\beta,j}}'$ and ${F_{\gamma,j}}'$ are the measured sample data of the random variables F_β and F_γ respectively for the jth measurement during a long measured time, and Z_F is the number of the measured samples of F_β and F_γ. In the above calculation equations, the mean values of noises are eliminated from the mean values of random variables F_β and F_γ respectively, and the influences of noises are suppressed. The formulas for calculating the ML estimator can be represented as follow:

$$\begin{cases} \frac{\partial}{\partial I_1}\left\{ln\left[\frac{1}{\sqrt{2\pi{\sigma_F}^2}}exp\left(-\frac{\left(F_\beta - m_{F_\beta}\right)^2}{2{\sigma_F}^2}\right)\frac{1}{\sqrt{2\pi{\sigma_F}^2}}exp\left(-\frac{\left(F_\gamma - m_{F_\gamma}\right)^2}{2{\sigma_F}^2}\right)\right]\right\} = 0 \\ \frac{\partial}{\partial I_1}\left\{ln\left[\frac{1}{\sqrt{2\pi{\sigma_F}^2}}exp\left(-\frac{\left(F_\beta - m_{F_\beta}\right)^2}{2{\sigma_F}^2}\right)\frac{1}{\sqrt{2\pi{\sigma_F}^2}}exp\left(-\frac{\left(F_\gamma - m_{F_\gamma}\right)^2}{2{\sigma_F}^2}\right)\right]\right\} = 0 \end{cases} \tag{11}$$

The following formulas can be obtained by using (8), (9), (10) and (11)

$$\begin{cases} \frac{1}{Z_F}\sum_{j=1}^{Z_F} {F_{\beta,j}}' = m_{F_\beta} \\ \frac{1}{Z_F}\sum_{j=1}^{Z_F} {F_{\gamma,j}}' = m_{F_\gamma} \end{cases} \tag{12}$$

The $\overrightarrow{\hat{\boldsymbol{I}}_{\boldsymbol{ML}}} = \left[\hat{I}_{1_{ML}} \quad \hat{I}_{2_{ML}}\right]$ can be calculated as follow by using (9), (10), (11) and (12).

$$\begin{cases} \hat{I}_{1_{ML}} = \frac{4f_1\left\{(M_8-M_9)\cdot J\cdot \overline{F_\gamma}' - [(u'-v')+(M_{13}-M_{14})]\cdot J'\cdot \overline{F_\beta}'\right\}}{J'J\{(M_8-M_9)(M_{11}-M_{12}) - [(u-v)+(M_6-M_7)][(u'-v')+(M_{13}-M_{14})]\}} \\ \hat{I}_{2_{ML}} = \frac{4f_2\left\{(M_{11}-M_{12})\cdot J'\cdot \overline{F_\beta}' - [(u-v)+(M_6-M_7)]\cdot J\cdot \overline{F_\gamma}'\right\}}{J'J\{(M_8-M_9)(M_{11}-M_{12}) - [(u-v)+(M_6-M_7)][(u'-v')+(M_{13}-M_{14})]\}} \end{cases} \tag{13}$$

This article has been accepted for publication in a future issue of this journal, but has not been fully edited. Content may change prior to final publication. Citation information: DOI 10.1109/ACCESS.2021.3110968, IEEE Access

IV. PERFORMANCE ANALYSIS

A. UNBIASED PROPERTY

The ML estimator $\overrightarrow{\hat{\boldsymbol{I}}_{\boldsymbol{ML}}} = [\hat{I}_{1_{ML}} \quad \hat{I}_{2_{ML}}]$ is proved to be unbiased by calculating the mean value $E\left(\overrightarrow{\hat{\boldsymbol{I}}_{\boldsymbol{ML}}}\right)$ of the ML estimate $\overrightarrow{\hat{\boldsymbol{I}}_{\boldsymbol{ML}}}$ as follow and by using (9), (10) and (13) :

$$\begin{aligned} E(\hat{I}_{1_{ML}}) &= E\left(\frac{4f_1\{(M_8-M_9)\cdot J\cdot \overline{F_\gamma}' - [(u'-v')+(M_{13}-M_{14})]\cdot J'\cdot \overline{F_\beta}'\}}{J'J\{(M_8-M_9)(M_{11}-M_{12})-[(u-v)+(M_6-M_7)][(u'-v')+(M_{13}-M_{14})]\}}\right) \\ &= \frac{4f_1\{(M_8-M_9)\cdot J\cdot E(\overline{F_\gamma}') - [(u'-v')+(M_{13}-M_{14})]\cdot J'\cdot E(\overline{F_\beta}')\}}{J'J\{(M_8-M_9)(M_{11}-M_{12})-[(u-v)+(M_6-M_7)][(u'-v')+(M_{13}-M_{14})]\}} \\ &= I_1 \end{aligned} \tag{14}$$

$$\begin{aligned} E(\hat{I}_{2_{ML}}) &= E\left(\frac{4f_2\{(M_{11}-M_{12})\cdot J'\cdot \overline{F_\beta}' - [(u-v)+(M_6-M_7)]\cdot J\cdot \overline{F_\gamma}'\}}{J'J\{(M_8-M_9)(M_{11}-M_{12})-[(u-v)+(M_6-M_7)][(u'-v')+(M_{13}-M_{14})]\}}\right) \\ &= \frac{4f_2\{(M_{11}-M_{12})\cdot J'\cdot E(\overline{F_\beta}') - [(u-v)+(M_6-M_7)]\cdot J\cdot E(\overline{F_\gamma}')\}}{J'J\{(M_8-M_9)(M_{11}-M_{12})-[(u-v)+(M_6-M_7)][(u'-v')+(M_{13}-M_{14})]\}} \\ &= I_2 \end{aligned} \tag{15}$$

B. ESTIMATOR EFFICIENCY AND CONSISTENCY

In order to quantify how optimal this ML estimator is with respect to the mean square error (MSE), the Cramer-Rao lower bound (CRB) on the estimation variance is derived and analyzed. Because of $\frac{\partial\{ln[p(\vec{F}|\vec{I})]\}}{\partial I_1}|_{I_1=\hat{I}_{1ML}} = 0$ and $\frac{\partial\{ln[p(\vec{F}|\vec{I})]\}}{\partial I_2}|_{I_2=\hat{I}_{2ML}} = 0$, the following formulas can be obtained:

$$\frac{\partial\{ln[p(\vec{F}|\vec{I})]\}}{\partial \vec{I}} = \begin{bmatrix} \frac{\partial\{ln[p(\vec{F}|\vec{I})]\}}{\partial I_1} \\ \frac{\partial\{ln[p(\vec{F}|\vec{I})]\}}{\partial I_2} \end{bmatrix} = -\begin{bmatrix} J_{11} & J_{12} \\ J_{21} & J_{22} \end{bmatrix}\begin{bmatrix} I_1 - \hat{I}_{1_{ML}} \\ I_2 - \hat{I}_{2_{ML}} \end{bmatrix} = \begin{bmatrix} 0 \\ 0 \end{bmatrix} \tag{16}$$

The Fisher information is calculated as follow for the unrelated I_1 and I_2:

$$\begin{cases} J_{11} = -E\left[\frac{\partial^2\{ln[p(\vec{F}|\vec{I})]\}}{\partial {I_1}^2}\right] = \frac{z_F}{{\sigma_F}^2}\left\{\frac{[(u-v)+(M_6-M_7)]^2J^2 + (M_{11}-M_{12})^2J'^2}{(4f_1)^2}\right\} \\ J_{22} = -E\left[\frac{\partial^2\{ln[p(\vec{F}|\vec{I})]\}}{\partial {I_{22}}^2}\right] = \frac{z_F}{{\sigma_F}^2}\left\{\frac{[(M_8-M_9)]^2J^2 + [(u'-v')+(M_{13}-M_{14})]^2J'^2}{(4f_2)^2}\right\} \end{cases} \tag{17}$$

The estimation signal noise ratio ρ_1 and ρ_2 can be represented as

$$\begin{cases} \rho_1 = \dfrac{\left\{\frac{[(u-v)+(M_6-M_7)]^2J^2 + (M_{11}-M_{12})^2J'^2}{(4f_1)^2}\right\}}{{\sigma_F}^2} \\ \rho_2 = \dfrac{\left\{\frac{[(M_8-M_9)]^2J^2 + [(u'-v')+(M_{13}-M_{14})]^2J'^2}{(4f_2)^2}\right\}}{{\sigma_F}^2} \end{cases} \tag{18}$$

The estimation mean square error ${\varepsilon_{\hat{I}_1}}^2$ and ${\varepsilon_{\hat{I}_2}}^2$ of the unrelated variables I_1 and I_2 can be obtained and are equal to the CRB as follow, which means the unbiased ML estimator $\overrightarrow{\hat{\boldsymbol{I}}_{\boldsymbol{ML}}} = [\hat{I}_{1_{ML}} \quad \hat{I}_{2_{ML}}]$ has the minimum mean square error. If the measurement number z_F and the estimation signal noise ratio ρ_1 and ρ_2 are increased and the estimation error can be decreased in practice.

$$\begin{cases} {\varepsilon_{\hat{I}_1}}^2 = \dfrac{1}{-E\left[\frac{\partial^2 ln[p(\vec{F}|\vec{I})]}{\partial {I_1}^2}\right]} = \dfrac{1}{\frac{z_F}{{\sigma_F}^2}\left\{\frac{[(u-v)+(M_6-M_7)]^2J^2 + (M_{11}-M_{12})^2J'^2}{(4f_1)^2}\right\}} \\ {\varepsilon_{\hat{I}_2}}^2 = \dfrac{1}{-E\left[\frac{\partial^2 ln[p(\vec{F}|\vec{I})]}{\partial {I_2}^2}\right]} = \dfrac{1}{\frac{z_F}{{\sigma_F}^2}\left\{\frac{[(M_8-M_9)]^2J^2 + [(u'-v')+(M_{13}-M_{14})]^2J'^2}{(4f_2)^2}\right\}} \end{cases} \tag{19}$$

$$\begin{cases} {\varepsilon_{\hat{I}_1}}^2 = \dfrac{1}{z_F\rho_1} \\ {\varepsilon_{\hat{I}_2}}^2 = \dfrac{1}{z_F\rho_2} \end{cases} \tag{20}$$

V. APPLICATION AND SIMULATION

The equivalent average amplitudes I_1 and I_2 can be obtained respectively by using the ICIDC statistical algorithm based on the FPA , in order to effectively eliminate the influence of the reflected optical signal on the signal detection, and to eliminate the pixel noise mean value from the expression of I_1 and I_2.

In an optical communication system including the terminal A and B, the FPA output of each terminal has the frame frequency $f_{frame} = 10kfps$, and $T_{frame} = \frac{1}{f_{frame}} = 100\mu s$. The working wavelength of the optical signal emitted by the terminal A is 1550nm, and its modulation signal $S_1(t)$ is the OOK modulated signal with the frequency $f_1 = 1.7MHz$, the duty cycle 50% and the equivalent average amplitudes I_1. The other parameters for the terminal A are $K = 10$, $(2M_1 + 1) = 17$, $K(2M_1 + 1) = 170$, $M_1 = 8$, $\frac{(2M_1+1)}{2} = 8.5$. The working wavelength of the optical signal emitted by the terminal B is 1551nm, and its modulation signal $S_2(t)$ is the OOK modulated signal with the frequency $f_2 = 1MHz$, the duty cycle 50% and the equivalent average amplitudes I_2. The other parameters for the terminal B is $K = 10$, $(2M_2) = 10$, $K(2M_2) = 100$, $M_2 = 5$, $\frac{(2M_2)}{2} = 5$. The incident optical signals for the terminal A include: (1) the reflected signal $S_1(t)$ that is emitted by the terminal A. (2) the receiving signal $S_2(t)$ that is transmitted by the remote terminal B. The system diagram for the optical terminal A including incident light signals is shown in Fig. 1. The integral control signal $S_{int}(t)$ is designed in (21) as the OOK modulation periodic signal with one period time of $T_{cycle} = 400\mu s$, which includes 4 frames, namely the R, $(R+1)$, $(R+2)$ and $(R+3)$ frames. Each frame time is $T_{frame} = 100\mu s$ and includes $K = 10$ time segments. It is assumed that the synchronization between the signal $S_2(t)$ and the local timing clock of the terminal A has been completed well and the reset time for each frame are ignorable for this FPA.

This article has been accepted for publication in a future issue of this journal, but has not been fully edited. Content may change prior to final publication. Citation information: DOI 10.1109/ACCESS.2021.3110968, IEEE Access

$$S_{int}(t)=\begin{cases}1\ [R\cdot 100\mu s+i\cdot 10\mu s]\le t<[R\cdot 100\mu s+i\cdot 10\mu s+5\mu s] & i=0,1\dots 9\\ 0\ [R\cdot 100\mu s+i\cdot 10\mu s+5\mu s]\le t<[R\cdot 100\mu s+(i+1)\cdot 10\mu s] & i=0,1\dots 9\\ 0\ [(R+1)\cdot 100\mu s+i\cdot 10\mu s]\le t<[(R+1)\cdot 100\mu s+i\cdot 10\mu s+5\mu s] & i=0,1\dots 9\\ 1\ [(R+1)\cdot 100\mu s+i\cdot 10\mu s+5\mu s]\le t<[(R+1)\cdot 100\mu s+(i+1)\cdot 10\mu s] & i=0,1\dots 9\\ 1\ [(R+2)\cdot 100\mu s+i\cdot 10\mu s]\le t<[(R+2)\cdot 100\mu s+i\cdot 10\mu s+3.53\mu s] & i=0,1\dots 9\\ 0\ [(R+2)\cdot 100\mu s+i\cdot 10\mu s+3.53\mu s]\le t<[(R+2)\cdot 100\mu s+i\cdot 10\mu s+6.47\mu s] & i=0,1\dots 9\\ 0\ [(R+2)\cdot 100\mu s+i\cdot 10\mu s+6.47\mu s]\le t<[(R+2)\cdot 100\mu s+(i+1)\cdot 10\mu s] & i=0,1\dots 9\\ 0\ [(R+3)\cdot 100\mu s+i\cdot 10\mu s]\le t<[(R+3)\cdot 100\mu s+i\cdot 10\mu s+3.53\mu s] & i=0,1\dots 9\\ 0\ [(R+3)\cdot 100\mu s+i\cdot 10\mu s+3.53\mu s]\le t<[(R+3)\cdot 100\mu s+i\cdot 10\mu s+6.47\mu s] & i=0,1\dots 9\\ 1\ [(R+3)\cdot 100\mu s+i\cdot 10\mu s+6.47\mu s]\le t<[(R+3)\cdot 100\mu s+(i+1)\cdot 10\mu s] & i=0,1\dots 9\end{cases} \tag{21}$$

By using the co-simulation of the OptiSystem and MATLAB software, the modulated signals of $S_1(t)$ and $S_2(t)$, and the FPA integral control signal $S_{int}(t)$ are generated, and the FPA detection system are built and simulated. The FPA output signals are obtained and the ICIDC statistical algorithm are programmed and calculated finally. The statistically calculated results of the equivalent average amplitudes I_1 and I_2 can be obtained respectively and clearly. The diagram of the optical detection simulation for the terminal A is shown in Fig. 3 and Fig. 4 as follow. Because of the page limitation, the synchronization of this method will be discussion in the future.

The 6X6 elements of FPA are simulated and the light spots of Gaussian beams from the terminal A and B are generated with the center power -50dBm, respectively. These two spots are overlapped in order to simulate one of the worst cases. The FPA integral output signal is shown in Fig. 5(a) and the FPA total received signals are shown in Fig. 5(b). The noise of each element is added to the FPA simulation system as a Gaussian random variable. By the ICIDC statistical algorithm, the equivalent average amplitudes I_1 and I_2 can be obtained more precisely, as shown in Fig. 5(c) and 5(d).

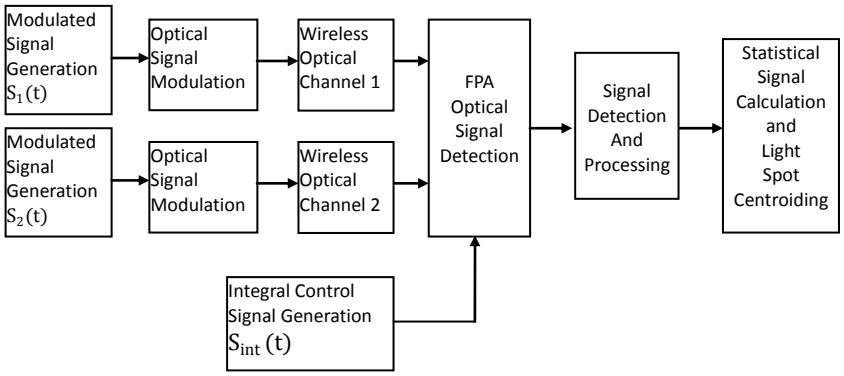

FIGURE 3. Block diagram of the optical detection simulation for the terminal A

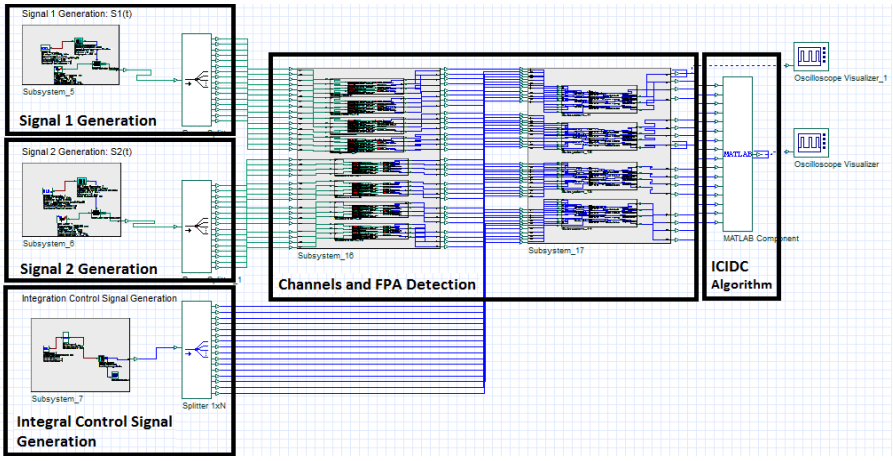

FIGURE 4. Simulation layout including the parts of the signal 1 and 2 generation, the wireless optical channels, the FPA detection, the integral control signal generation and the ICIDC algorithm.

This article has been accepted for publication in a future issue of this journal, but has not been fully edited. Content may change prior to final publication. Citation information: DOI 10.1109/ACCESS.2021.3110968, IEEE Access

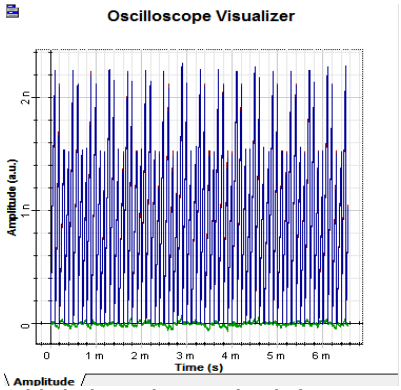

(a) The integral output signal of FPA

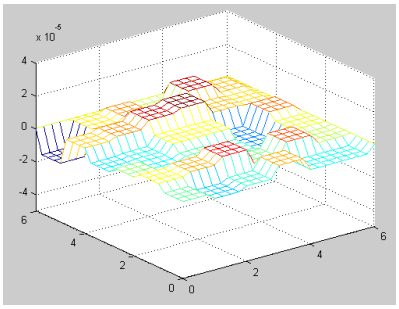

(b) FPA total received signal

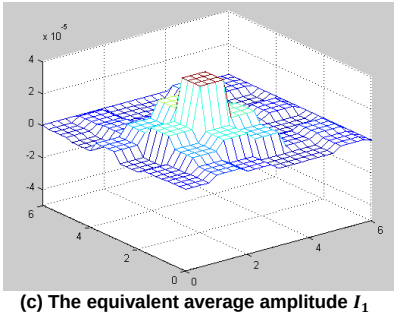

(c) The equivalent average amplitude I_1

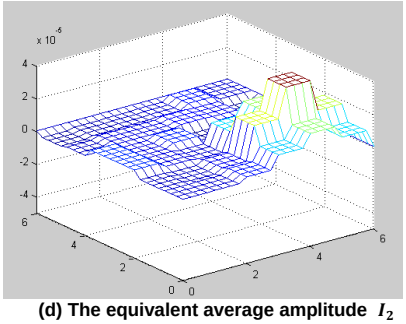

(d) The equivalent average amplitude I_2

FIGURE 5. Diagram of simulation results

VI. CONCLUSION

In this paper, an ICIDC statistical algorithm for FPAs is proposed, the statistical models of this method are made, the calculation formulas are obtained, and the CRB performance is analyzed. In addition, the software co-simulation of the FPA detection system is built and the statistical algorithms are implemented. In the simulation, the results of the equivalent average amplitudes $\boldsymbol{I_1}$ and $\boldsymbol{I_2}$ are obtained more precisely. The feasibility and validity of the ICIDC method are verified by the simulation and the advantages of the ICIDC method are analyzed, e.g the effective elimination of the influence of reflected optical signal on the receiving optical signal detection and the noise mean part in the mean value of detection signal. This method can improve the detection sensitivity, path isolation and spot centroid calculation accuracy of the FPA.

REFERENCES

[1] H. Hemmati, "Deep-Space Communications and Navigation Series", JPL, Wiley, 2006.

[2] H. P. Hsu, "Schaum's Outline of Theory and Problems of Probability, Random Variables, and Random Processes", ser. Schaum's Outline. McGraw-Hill Companies, Inc., 1997

[3] Meera Srinivasan, Ryan Rogalin, and Norman Lay, *et al.*, "Downlink Receiver Algorithms for Deep Space Optical Communications," Free-Space Laser Communication and Atmospheric Propagation XXIX, Proc. of SPIE, vol. 10096, 100960A, 2017, doi: 10.1117/12.2254887.

[4] Abhijit Biswas, Hamid Hemmati, Sabino Piazzolla, *et al.*, "Deep-space Optical Terminals (DOT) Systems Engineering," NASA IPN Progress Report 42-183A, November 15, 2010 .

[5] Guy Baister, Thomas Dreischer, and Michael Tüchler, et al., "OPTEL Terminal for Deep Space Telemetry Links," Free-Space Laser Communication Technologies XIX and At mospheric Propagation of Electromagnetic Waves, Proc. of SPIE, vol. 6457, 645706-3, 2007, doi: 10.1117/12.708770.

XIAOYAN WANG received the Ph.D. degree in electrical engineering from the University of Nevada, Reno, NV, USA, in 2011. She is currently with China Academy of Space Technology (Xi'an), Xi'an, Shaanxi, China. Her research interests include deep space optical communications, near-earth laser communications and integrated optical and RF space communications.

YUNING WANG received the B.S. degree in information engineering from Xi'an Jiaotong University, Xi'an, China, in 2019. She is currently pursuing the Ph.D. degree in control science and engineering from Xi'an Jiaotong University, Xi'an, Shaanxi, China. Her research interests include signal processing and machine learning application for wireless communications.

LI LI is currently a Research Fellow of China Academy of Space Technology (Xi'an) and has long been engaged in the research and project development of space data processing and transmission, and advanced satellite payload technology. He had presided over more than 10 national projects and obtained 25 national invention patents. He has successively won the second-class National Science and Technology Progress Award thrice, the first-class of Science and Technology Progress Award of the Ministry of Education once and the National Defense Science and Technology Progress Award many times.

JIANHUA ZHANG is a Research Fellow of China Academy of Space Technology (CAST) (Xi'an) and is currently the Director of the Institute of Space Data Transmission and Procession in CAST. His current research interests include satellite communications, laser communications, software-defined radio system and space networking.

ZHOUSHI YAO, Ph.D., joined China Academy of Space Technology (CAST) (Xi'an) in 2008 as the director of National Key Laboratory on Space Microwave Technology, and was the Deputy Director of the Institute of Space Data Transmission and Procession in 2013. He has been the Principal Investigator of the Laser Communications of CAST Xi'an for nearly 13 years until he joined Zhejiang University in 2021 as the Director Professor of Sat-Internet Research Group within the school of Aeronautics and Astronautics.

CHANGZHI XU received the B.S. degree in electronic information engineering from Xidian University, Xi'an, China, in 2006, and M.S. degree in biomedical engineering from Xidian University, Xi'an, China, in 2009. He is currently pursuing the Ph.D. degree with State Key Laboratory of Millimeter Waves, Southeast University, Nanjing, China. He is with the China Academy of Space Technology (Xi'an), Xi'an, China. His research interests include satellite communications, laser communications and software defined radio system.

YI JIN received the B.S. degree in communication and information engineering from Nanjing University of Information Science and Technology, Nanjing, China, in 2005, and the Ph.D. degree in communication and information engineering from Southeast University, Nanjing, China, in 2013. He is currently with China Academy of Space Technology (Xi'an), Xi'an, China. His research interests include communication signal processing, satellite communications and networking.